Cytotherapy 000 (2022) 1–13

Contents lists available at ScienceDirect

CYTOTHERAPY

journal homepage: www.isct-cytotherapy.org

Full-length article

Bone marrow-derived inducible microglia-like cells ameliorate motor function and survival in a mouse model of amyotrophic lateral sclerosis

Shuhei Kobashi[1,2], Tomoya Terashima[1,*], Miwako Katagi[1], Makoto Urushitani[2], Hideto Kojima[1]

[1] Department of Stem Cell Biology and Regenerative Medicine, Shiga University of Medical Science, Otsu, Japan
[2] Department of Neurology, Shiga University of Medical Science, Otsu, Japan

ARTICLE INFO

Article History:
Received 4 November 2021
Accepted 3 February 2022
Available online xxx

Key Words:
amyotrophic lateral sclerosis
BM-iMG cells
bone marrow-derived cells
GM-CSF
IL-4
neuroprotective microglia

ABSTRACT

Background aims: Amyotrophic lateral sclerosis (ALS) is an incurable neurodegenerative disease. Neuroinflammation in the spinal cord plays a pivotal role in the pathogenesis of ALS, and microglia are involved in neuroinflammation. Microglia mainly have two opposite phenotypes involving cytotoxic and neuroprotective properties, and neuroprotective microglia are expected to be a novel application for the treatment of ALS. Therefore, to establish a clinically applicable therapeutic method using neuroprotective microglia, the authors investigated the effect of inducing neuroprotective microglia-like cells from bone marrow for transplantation into ALS model mice.

Methods: Bone marrow-derived mononuclear cells were isolated from green fluorescent protein mice and cultured using different protocols of cytokine treatment with granulocyte-macrophage colony-stimulating factor (GM-CSF) and IL-4. Cells with a high potency of proliferation and differentiation into microglia were evaluated by gene analysis, flow cytometry and direct neuroprotective effects *in vitro*. These cells were named bone marrow-derived inducible microglia-like (BM-iMG) cells and transplanted into the spinal cords of ALS model mice, and behavioral tests, immunohistochemistry and gene expression profiling were performed.

Results: Three-day GM-CSF and 4-day GM-CSF + IL-4 stimulations were most effective in inducing BM-iMG cells from the bone marrow. Transplantation of BM-iMG cells improved motor function, prolonged survival and suppressed neuronal cell death, astrogliosis and microgliosis in the spinal cords of ALS mice. Moreover, neuroprotective genes such as *Arg1* and *Mrc1* were upregulated, whereas pro-inflammatory genes such as *Nos2* and *Il6* were downregulated.

Conclusions: Intraspinal transplantation of BM-iMG cells demonstrated therapeutic effects in a mouse model of ALS. Further studies and clinical applications in patients with ALS are expected in the future.

Introduction

Amyotrophic lateral sclerosis (ALS) is a neurodegenerative disease characterized by progressive motor dysfunction, owing to motor neuron death, and a poor prognosis for which there is no curative therapy [1]. Emerging evidence indicates that the accumulation of pathogenic proteins in the central nervous system (CNS) is implicated in the pathogenesis of ALS. Moreover, inflammation is crucial in ALS and other neurological diseases, such as multiple sclerosis and spinal cord injury [2–4]. Infiltrates of inflammatory lymphocytes have been reported in the spinal cords of patients with ALS [4]. Microglial activation has been observed prior to lymphocyte infiltration, which induces neurotoxic effects by producing tumor necrosis factor alpha, IL-1β and reactive oxygen species, in an ALS mouse model [5–7].

Microglia are involved in maintaining homeostasis, regulating immune responses and removing foreign substances in the CNS [8,9]. Microglia are classically classified into two major phenotypes, pro-inflammatory and neuroprotective, which are involved in the pathogenesis of various neurological disorders [10–14]. In a mouse model of ALS, it has been reported that the phenotype of microglia in the spinal cord shifts from a neuroprotective-dominant phenotype to a pro-inflammatory-dominant phenotype as the disease progresses [15,16].

The authors have documented that bone marrow transplantation-based cell therapies are effective in prolonging survival and inhibiting the progression of motor dysfunction in ALS model mice by

* Correspondence: Tomoya Terashima, MD, PhD, Department of Stem Cell Biology and Regenerative Medicine, Shiga University of Medical Science, Seta Tsukinowa-cho, Otsu 520-2192, Japan.
E-mail address: tom@belle.shiga-med.ac.jp (T. Terashima).

https://doi.org/10.1016/j.jcyt.2022.02.001

suppressing neuroinflammation [17–19]. In these studies, bone marrow cells were differentiated into microglia-like cells and endowed with neuroprotection, suggesting the promising therapeutic potential of bone marrow cells. Furthermore, direct transplantation of neuroprotective microglia into the spinal cord after a traumatic injury results in functional recovery by amelioration of neuroinflammation [20]. These results prompted the authors to apply neuroprotective microglia in the treatment of ALS. However, when considering clinical application, it is a technical and ethical hurdle to obtain a large amount of neuroprotective microglia for transplantation or primary microglial culture cells from the human embryonic brain. Therefore, the authors focused on bone marrow-derived mononuclear cells (BM-MNCs) and established an induction strategy for generating neuroprotective microglia from BM-MNCs, which were named bone marrow-derived inducible microglia-like (BM-iMG) cells. In this study, BM-iMG cells were transplanted into the spinal cords of ALS mice, and their effects on neuroinflammation and phenotypes were investigated.

Methods

Animals

C57BL/6, h superoxide dismutase (SOD) 1 (G93A) 1Gur/J with a high copy number of mutant SOD1 (SOD1-tg mice) and C57BL/6-Tg (UBC–green fluorescent protein [GFP]) 30Scha/J (GFP-tg mice) were purchased from The Jackson Laboratory (Bar Harbor, ME, USA) and prepared for the animal experiments. Male SOD1-tg mice show disease onset at around 90 days and die at 120–140 days after birth. As the copy number of mutant *SOD1* gene is known to be reduced in some pedigrees by repeated breeding, mice >160 days old and their littermates were excluded from the succession of the next generation. Mouse chow and water were provided to all animals ad lib, and mice were maintained under a 12-h light–dark cycle. Animal experimental protocols (2016-11-10 and 2016-11-10-H1) were approved by the institutional animal care and use committee at Shiga University of Medical Science. In addition, all animal experiments were carried out in accordance with the institutional animal care and use committee guidelines at Shiga University of Medical Science; the National Research Council's Guide for the Care and Use of Laboratory Animals, published by the United States National Institutes of Health; and the Animal Research: Reporting of *In Vivo* Experiments guidelines.

Isolation of bone marrow and induction of BM-iMG cells from mice

Both sides of the tibia and femur were isolated from the C57BL/6, GFP-tg or SOD1-tg adult mice and disinfected with 70% ethanol. These bones were cut at both ends, and bone marrow was pressed out with phosphate-buffered saline (PBS) and a 5-mL syringe filled with a 25-gauge needle. The extruded bone marrow was passed through a 70-μm filter and washed. Finally, bone marrow cells were resuspended in 5 mL of PBS. The authors were usually able to harvest a total of $2–3 \times 10^7$ nucleated bone marrow cells from each mouse. Additionally, $5–6 \times 10^6$ BM-MNCs were isolated from the nucleated bone marrow cells obtained from each mouse using 5 mL Ficoll-Paque PLUS gradient separation (GE Healthcare Bio-Sciences AB, Uppsala, Sweden). The isolated BM-MNCs were cultured in a 35-mm culture dish with 3 mL StemSpan Serum-Free Expansion Medium (STEMCELL Technologies, Vancouver, Canada) at a concentration of 10^5 cells/mL for 7 days with granulocyte-macrophage colony-stimulating factor (GM-CSF) (Wako Pure Chemical Industries, Ltd, Osaka, Japan) and/or IL-4 (Wako Pure Chemical Industries, Ltd) using the following methods: GM-CSF 40 ng/mL for 7 days (method A), GM-CSF 40 ng/mL + IL-4 at 40 ng/mL for 7 days (method B) and 40 ng/mL GM-CSF for 3 days followed by GM-CSF 40 ng/mL + IL-4 at 40 ng/mL for 4 days (method C). The authors were able to prepare approximately twenty 35-mm dishes from one mouse. For all methods, the culture medium was replaced with fresh medium on day 3. After 7 days, the cultured cells were observed under optical microscope. Additionally, these cells were treated with trypsin–ethylenediaminetetraacetic acid (EDTA) (Life Technologies, Carlsbad, CA, USA) for 10 min, collected by scraping and counted to calculate the growth rate of the seeded cells.

Flow cytometry analysis of BM-iMG cells

BM-MNCs isolated from C57BL/6 and SOD1-tg mice were cultured using methods A, B and C for 7 days. These cells were treated with trypsin-EDTA for 10 min and collected by scraping. The collected cells were stained with fluorescein isothiocyanate–CD11b antibody (BD Biosciences, Franklin Lakes, NJ, USA), phycoerythrin–CD86 antibody (BD Biosciences) and Alexa Fluor 647-CD206 antibody (BioLegend, San Diego, CA, USA) and analyzed for surface antigens by flow cytometry. To confirm that BM-iMG cells did not include the CD45-negative fraction represented by mesenchymal stem cells, the cells were also stained with fluorescein isothiocyanate–CD45 antibody (BD Biosciences) and checked to show CD45 positivity. Data were collected using a FACSCalibur or FACSAria flow cytometer (BD Biosciences).

Neuronal cell viability assay

BM-MNCs were cultured using method C, and the supernatants were collected as the conditioned medium. StemSpan medium with GM-CSF 40 ng/mL + IL-4 40 ng/mL without the cells was placed in a carbon dioxide incubator at 37°C for 4 days as a control medium. The motor neuron cell line NSC-34 was purchased from CELLutions Biosystems (Burlington, Canada). These cells were seeded in a 96-well plate at 3×10^4 cells/well in high-glucose Dulbecco's Modified Eagle's Medium (DMEM) (Wako Pure Chemical Industries, Ltd) supplemented with 10% fetal bovine serum for 3 h. After confirming that the cells were adherent, the supernatant was changed to 60 μL high-glucose DMEM mixed with 40 μL of conditioned or control medium. Subsequently, 1-hydroxy-2-oxo-3,3-bis(2-aminoethyl)-1-triazene (NOC-18; Dojindo Molecular Technologies, Inc, Kumamoto, Japan) was added at 400 μM and incubated at 37°C for 48 h in a carbon dioxide incubator to induce neuronal cell death. Consequently, the supernatant was replaced with high-glucose DMEM supplemented with 10% fetal bovine serum.

The survival rates of NSC-34 cells were measured using Cell Counting Kit 8 (Dojindo Molecular Technologies, Inc) according to the manufacturer's protocol. Initially, 10 μL WST-8, which is included in the kit, was added to each well. WST-8 received a reduction reaction by dehydrogenase in live cells and developed orange color by changing to WST-8 formazan. Absorbance of the orange color was detected at a wavelength of 450 nm using an Infinite F200 multi-well plate reader (Tecan Japan Co, Ltd, Kawasaki, Japan). The absorbance ratio in each group was calculated by standardization with the absorbance of the control group after 48 h of treatment.

Transplantation of BM-iMG cells for SOD1-tg mice

Wild-type BM-MNCs isolated from GFP-tg mice were cultured using method C as BM-iMG cells. These cells were treated with trypsin-EDTA for 10 min and collected by scraping. The collected cells were counted and adjusted to 1.0×10^5 cells/μL in PBS. For the transplantation experiments, male SOD1-tg mice were used because males are heavier than females at the same age, they are resistant to physical stress and dehydration by surgery and their symptoms are more severe than those observed in females. SOD1-tg male mice aged 10 weeks were anesthetized with intraperitoneal injections of medetomidine (0.3 mg/kg), midazolam (4 mg/kg) and butorphanol (5 mg/

kg). The T13 vertebra of these mice, along with the surrounding skin, was then identified and disinfected with 70% ethanol. A skin incision of approximately 1 cm was made vertically with a scalpel, which was inserted horizontally into the intervertebral disc between the T12 and T13 vertebrae. Ophthalmic scissors were carefully inserted into the exposed region to avoid damage to the spinal cord, the left and right sides of the T13 vertebra were incised and the spinal cord was exposed by turning the T13 vertebra upward.

Next, the mice were fixed using a stereotactic device (Muromachi Kikai Co, Ltd, Tokyo, Japan). A 30-gauge needle was attached to a Hamilton syringe (Hamilton, Reno, NV, USA) filled with the prepared cell solution, and the needle was inserted 250 μm laterally from the midline of the spinal cord to a depth of 1 mm at a position between the T13 and L1 vertebrae. A total of 3 min following the puncture, 1 μL of the prepared cell solution was injected slowly into the spinal cord for 1 min. A total of 3 min following administration, the needle was withdrawn and the same procedure was performed on the other side of the spinal cord. A total of 2×10^5 BM-iMG cells were injected into the spinal cord of each male SOD1-tg mouse. The control group was injected with PBS in the same manner. After these procedures, the spine was restored at the original position and subcutaneous tissues were sutured vertically with 6-0 nylon to fix the spine. The skin was sutured using 5-0 nylon. Mice that showed weight loss >15% from the previous week were immediately euthanized in the interests of animal welfare.

Behavior test

After transplantation of BM-iMG cells, motor performance of the transplanted mice was analyzed using rotarod tests (Ugo Basile, Gemonio, Italy) once every week, and body weight was measured at the same frequency. Physiological death was defined as the time at which the results of the rotarod tests yielded 0 seconds. The rotarod tests were performed at 5–50 rpm/min for 5 min (acceleration, 9 rpm/min^2). The means of three medians of five trials for each time point were calculated in each mouse and used for analysis. For the Kaplan–Meier survival curve, the number of surviving mice was counted until all mice were recognized as having undergone physiological death.

Histological analysis

Three weeks after the transplantation of BM-iMG cells or at the end-stage of ALS, mice were fixed by transcardial perfusion with 4% paraformaldehyde in 0.1 M PBS. After isolation of the spinal cord, sections of the spinal cord were cut using a cryostat at a thickness of 10 μm. For immunohistochemistry, sections were incubated with a primary antibody (rabbit anti-β3-tubulin [Cell Signaling Technology, Danvers, MA, USA], rabbit anti-Iba-1 [Wako Pure Chemical Industries, Ltd] or rabbit anti-glial fibrillary acidic protein (GFAP) [Cell Signaling Technology]) overnight at 4°C. The sections were further incubated with a secondary antibody (goat anti-rabbit Alexa 555 [Life Technologies, Carlsbad, CA, USA]) at 20–25°C for 4 h and mounted with VECTASHIELD with 4′,6-diamidino-2-phenylindole (Vector Laboratories, Inc, Burlingame, CA, USA).

Over five sections of spinal cords with a 50-μm interval per sample were observed using a FV1000-D confocal laser microscope (Olympus, Tokyo, Japan) for quantitative evaluation. To evaluate Iba-1 or GFAP staining, the number of cells positively stained with Alexa Fluor 555 was counted, the fluorescence intensity of Alexa Fluor 555 at the ventral horn was measured and the background value was subtracted using ImageJ v.1.52h (National Institutes of Health, Bethesda, MD, USA). For evaluation of survival motor neurons, cells with a size >400 μm^2 cell bodies stained with β3-tubulin in the ventral horn were considered alpha motor neurons and were counted in each section of spinal cords.

Reverse transcription–quantitative polymerase chain reaction analysis

For *in vitro* gene expression analysis, BM-MNCs were cultured using methods A, B and C, and their total RNA was extracted using the RNeasy kit protocol (QIAGEN, Valencia, CA, USA). The extracted RNA was used as a template, and reverse transcription was performed using the PrimeScript RT reagent kit (Takara Bio Inc, Kusatsu, Japan). Real-time polymerase chain reaction was performed using LightCycler 480 SYBR Green I Master (Roche Diagnostics GmbH, Mannheim, Germany) with a LightCycler 480 (Roche Diagnostics GmbH). *In vivo* gene expression analysis was performed 3 weeks after transplantation of BM-iMG cells or at the end-stage of ALS by isolating the spinal cords of SOD1-tg mice after removal of blood by transcardial perfusion with 0.1 M PBS. Total RNA for analysis was extracted from the spinal cord using an RNeasy kit. Reverse transcription and real-time polymerase chain reaction was performed in the same manner as that described for the *in vitro* method.

The following primers were used: *Gapdh* forward primer, 5'-ATGACCACAGTCCATGCCATC-3', and reverse primer, 5′-GAGCTTCCCGTTCAGCTCTG-3′; *Cd86* forward primer, 5′-CACGAGCTTTGACAGGAACA-3′, and reverse primer, 5′-TTAGGTTTCGGGTGACCTTG-3′; *Mrc1* forward primer, 5′-CTATGCAGGCCACTGCTACA-3′, and reverse primer, 5′-GTTCTCATGGCTTGGCTCTC-3′; *Nos2* forward primer, 5′-TTGGAGCGAGTTGTGGATTG-3′, and reverse primer, 5′-GTAGGTGAGGGCTTGGCTGA-3′; *Arg1* forward primer, 5′-ACCTGCTGGGAAGGAAGAAAAG-3′, and reverse primer, 5′-GTTCCGAAGCAAGCCAAGGT-3′; *Il-6* forward primer, 5′-ACGGCCTTCCCTACTTCACA-3′, and reverse primer, 5′-CATTTCCACGATTTCCCAGA-3′; tumor necrosis factor alpha forward primer, 5′-CACGTCGTAGCAAACCACCAAGTGG-3′, and reverse primer, 5′-GATAGCAAATCGGCTGACGGTGTGG-3′; and β-*actin* forward primer, 5′-CGTGCGTGACATCAAAGAGAA-3′, and reverse primer, 5′-TGGATGCCACAGGATTCCAT-3′. All data were normalized to β-*actin* as housekeeping gene, and the results were analyzed using LightCycler 480 software, version 1.5 (Roche Diagnostics GmbH).

Statistical analysis

Data are expressed as mean ± standard deviation. For all multiple datasets, one-way or two-way analysis of variance was performed, followed by Tukey test for post-hoc statistical analysis. For behavioral tests and body weight, datasets were analyzed using Bonferroni test at each time point after analysis of linear mixed model for repeated measures analysis of variance. The log-rank test was performed for analysis of the Kaplan–Meier curve. A $P < 0.05$ was set as statistically significant. All statistical analyses were performed using SPSS Statistics 25 (IBM Corporation, Armonk, NY, USA).

Results

Induction of neuroprotective microglia-like cells from BM-MNCs

First, the authors estimated the culture protocol to optimize the cells for transplantation. BM-MNCs were isolated from adult C57BL/6 mice and cultured for 7 days with different combinations of GM-CSF with or without IL-4 using three methods (Figure 1A). After 7 days of culture, the features of these cells were analyzed for their proliferation and messenger RNA (mRNA) expression (Figure 1B,C). The number of cells after 7 days of culture was significantly increased with all methods compared with the number of seeded cells (Figure 1B). Moreover, the proliferation ratio over the 7 days was markedly high with methods A and C, which demonstrated a significantly higher ratio than that observed with method B. Further, the mRNA expression of *Arg1* and *Nos2*, markers for neuroprotective and pro-inflammatory microglia, respectively, was evaluated. The expression of *Arg1* was significantly elevated with method C compared with methods A

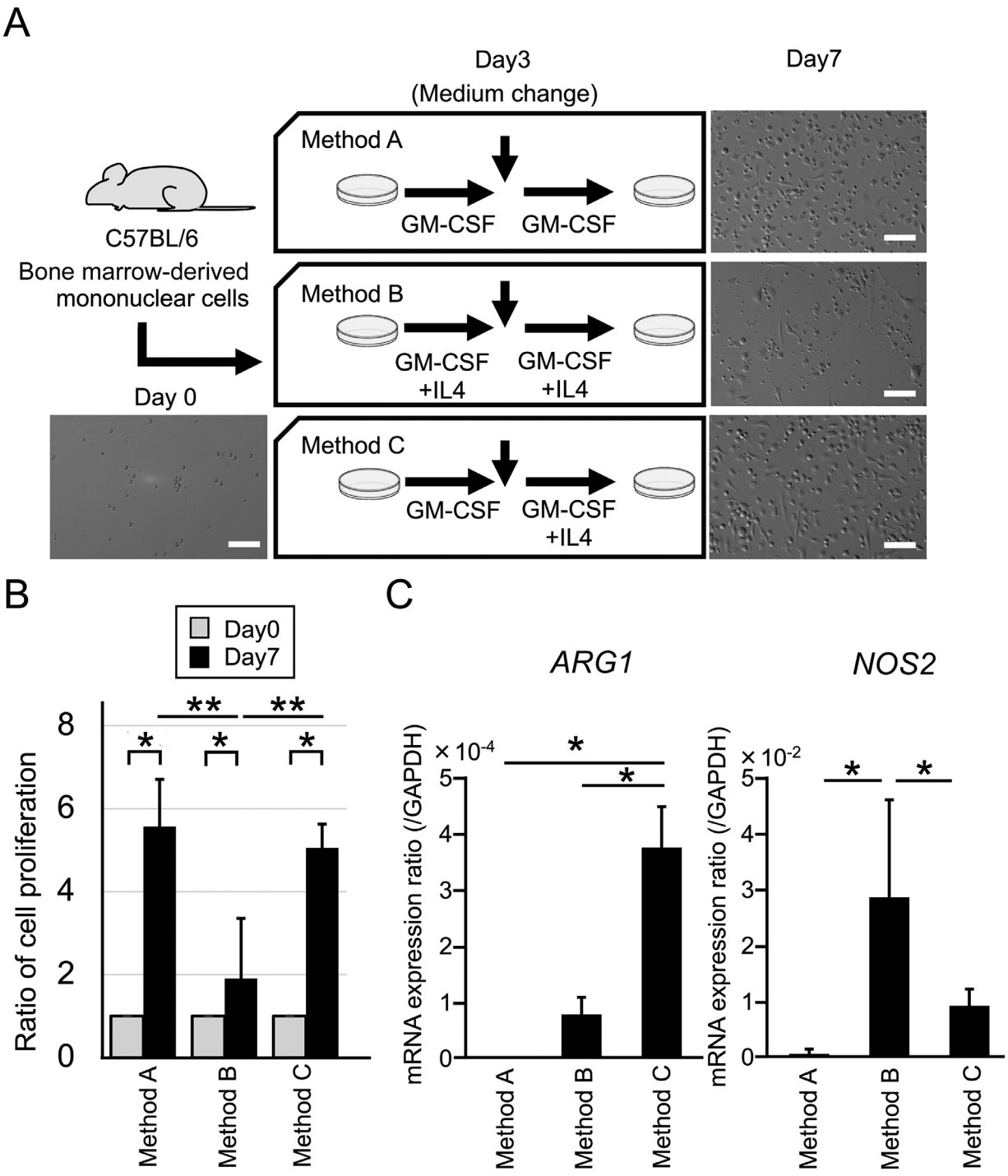

Figure 1. Differentiation of cultured BM-MNCs to inducible microglia-like cells with neuroprotective phenotype. (A) Three schematic strategies (methods A–C) for the differentiation of BM-MNCs cultured with a combination of GM-CSF and IL-4. Lower left panel shows the pre-cultured BM-MNCs at day 0. Right three panels show the cultured BM-MNCs at day 7 after incubation using method A (3-day GM-CSF and another 4-day GM-CSF stimulation), method B (3-day GM-CSF + IL-4 and another 4-day GM-CSF + IL-4 stimulation) or method C (3-day GM-CSF and another 4-day GM-CSF + IL-4 stimulation). Scale bars = 100 μm. (B) Proliferation ratio of cultured cells after incubation with methods A–C. Error bars show mean ± SD (n = 5 in each group). (C) Analysis of mRNA expression in the cultured BM-MNCs of the three groups. Bar graphs show the relative mRNA expression of *Arg1* and *Nos2* against the *Gapdh* gene. Error bars show mean ± SD (n = 5 in each group). $^{*}P < 0.05$, $^{**}P < 0.01$. SD, standard deviation.

and B. Additionally, the expression of *Nos2* was significantly elevated with method B compared with the other methods and was relatively maintained, without a marked increase, with method C (Figure 1C). These results suggested that, of the three methods, method C was the most suitable for inducing and obtaining a sufficient number of neuroprotective microglia.

Anti-inflammatory and neuroprotective properties of BM-iMG cells

After 7-day culture of BM-MNCs, expression of the surface antigens of microglia cultured using method C was analyzed by flow cytometry (Figure 2). For flow cytometry, the authors analyzed CD11b, CD206 and CD86 as markers for pan-macrophage/microglia,

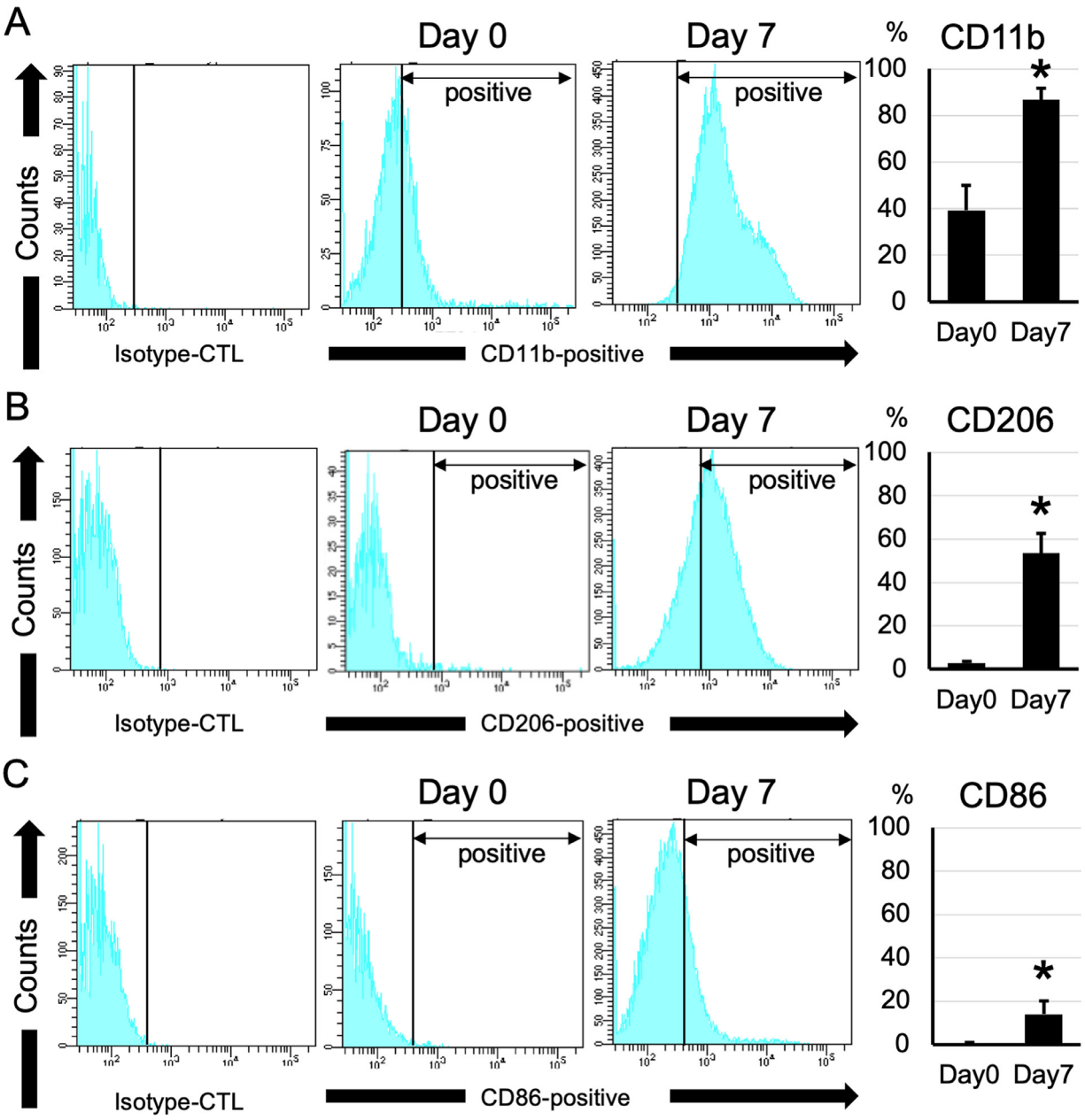

Figure 2. Flow cytometry analysis of BM-iMG cells with method C. (A) Light blue plots show the distribution of cell counts in a CD11b-positive population of BM-MNCs after incubation using method C. Most left panel shows the distribution of negative CTL with isotype-matched CTL antibody. Vertical black line in the plot indicates the threshold for the CD11b-positive population. The percentages of CD11b-positive cells in the two right blue plots (day 0 and day 7) were calculated by considering the right-sided population of the vertical black line as positive. Bar graph in most right panel shows the ratio of CD11b-positive cells at day 0 and day 7 after method C stimulation. Error bars show mean ± SD (n = 4 in each group). (B,C) Flow cytometry analysis of CD206 (B) and CD86 (C) antibodies. Both antibody-positive populations were analyzed before and after incubation using method C in the same manner as that used for (A). Error bars show mean ± SD. $^*P < 0.05$ vs day 0 group. CTL, control; SD, standard deviation.

neuroprotective microglia and pro-inflammatory microglia, respectively. The microglial population positive for both CD11b and CD206 significantly increased to over 50% on day 7 (Figure 2A,B). By contrast, the population of CD86-positive cells was slightly elevated, albeit still <20% (Figure 2C). Additionally, the population of CD11b-, CD206- and CD86-positive cells demonstrated comparative trends among the three methods (see supplementary Figure 1). Based on these results, the authors concluded that the cells cultured using method C possessed the most neuroprotective microglia-like phenotype. In addition, to confirm the purity of these cell populations, the authors investigated whether the CD45-negative population, as the mesenchymal stem cell fraction, was contaminated with the inducible cell fraction, and the level of contamination was found to be <1% (see supplementary Figure 2). The authors thus designated these cells BM-iMG cells.

Neuroprotective effects of BM-iMG cells in vitro

To confirm the neuroprotective effects of BM-iMG cells *in vitro*, the cell viability of NCS-34 cells, a motor neuron cell line, was analyzed in the presence or absence of conditioned medium from BM-iMG cell culture using the WST-8 assay (Figure 3A). The authors confirmed a positive correlation between cell density and WST-8 in NSC-34 cells (see supplementary Figure 3A). In addition, through preliminary experiments to evaluate the toxicity of NOC-18, a nitric oxide donor, as a chronic oxidative stressor, the authors determined

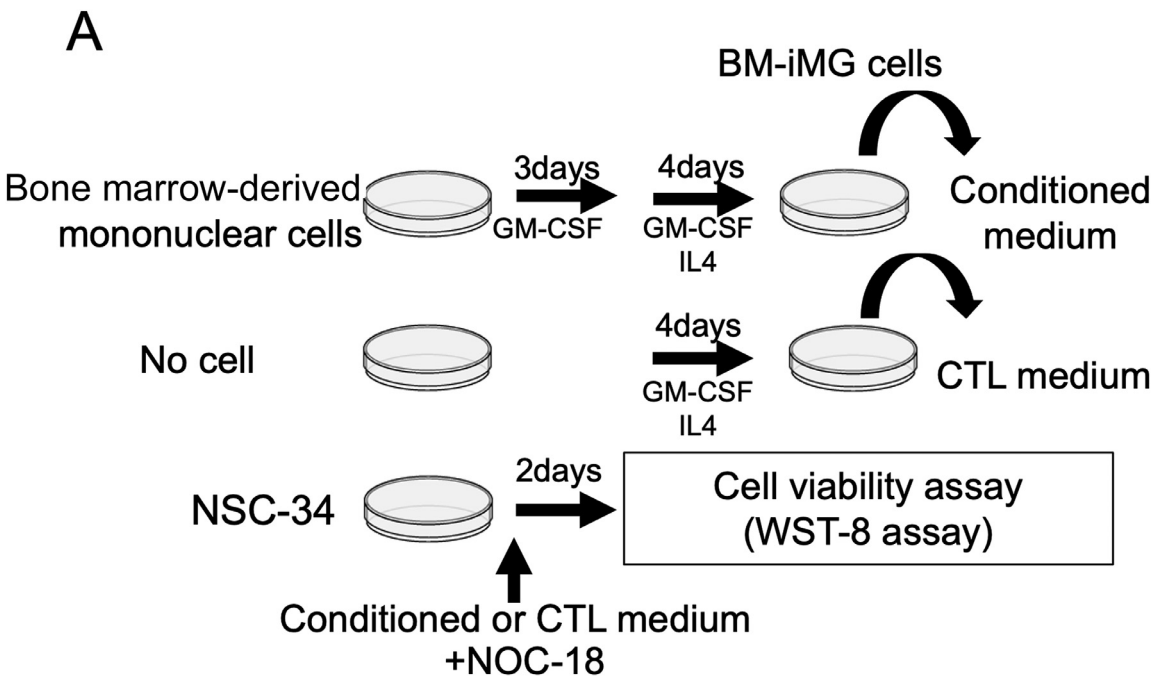

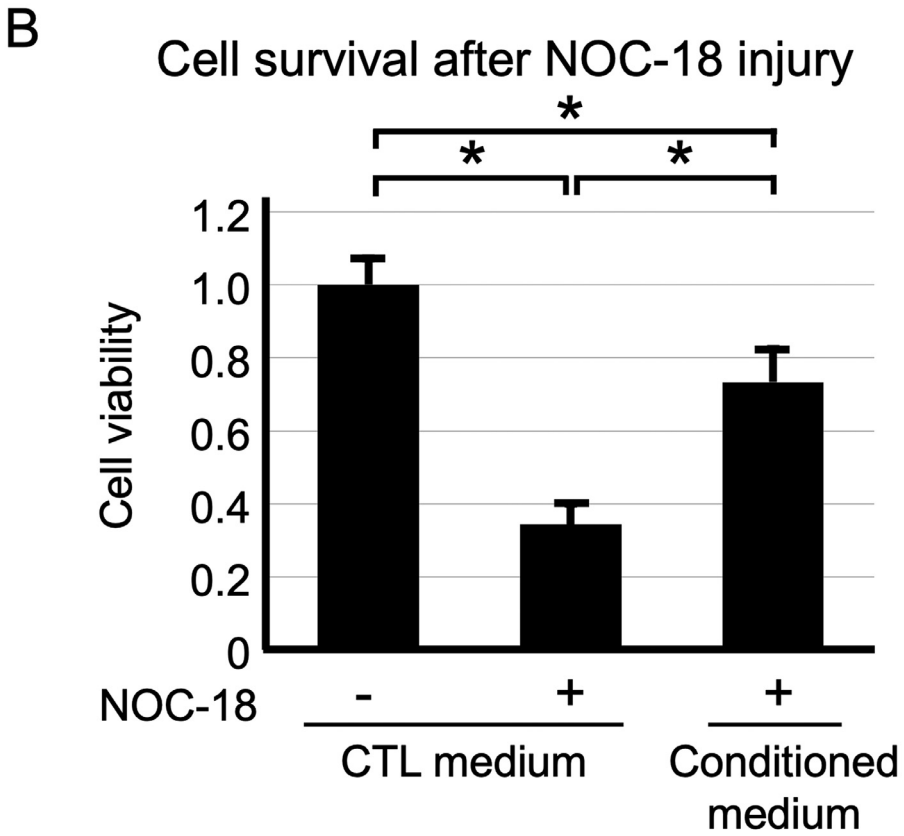

Figure 3. Neuroprotective effects of BM-iMG cells in NSC-34 cells. (A) Schematic presentation of experimental design. Conditioned medium was harvested from the supernatant of cultured BM-iMG cells with 3-day GM-CSF and another 4-day GM-CSF + IL-4 incubation. CTL medium was prepared without cell culture and with incubation of GM-CSF + IL-4 for 4 days. Viability of NCS-34 cells was analyzed by WST-8 assay 2 days after conditioned and CTL media were applied to NSC-34 cells under cell injury by NOC-18. (B) Viability of NCS-34 cells under NOC-18 injury with conditioned or CTL medium. Error bars show mean ± SD. $^*P < 0.05$. CTL, control; SD, standard deviation.

the optimal concentration of NOC-18 to be 400 μm^2, which demonstrated toxicity in >50% of NSC-34 cells and was appropriate for investigating the protective effect of BM-iMG-conditioned medium in NOC-18-induced neurotoxicity (see supplementary Figure 3A,B). After a 2-day exposure to NOC-18, replacement of the BM-iMG-conditioned medium significantly protected against the cytotoxic effects of NOC-18, whereas the control medium had no effect (Figure 3B).

Furthermore, as a study considering the possibility of autologous transplantation from ALS patients themselves, BM-MNCs were

isolated from adult SOD1-tg mice rather than wild-type mice and cultured for 7 days using method C. The number of nucleated bone marrow cells and BM-MNCs from SOD1-tg mice was almost the same as that from C57BL/6 wild-type mice (see supplementary Figure 4A,B). However, compared with wild-type BM-iMG cells, BM-iMG cells from SOD1-tg mice did not show a high proliferation ratio, with the ratio remaining similar to that observed with the initial cell number on day 0 (see supplementary Figure 4C). In addition, although the population of CD11b- and CD206-positive cells was similar between the wild-type and SOD1-tg groups (see supplementary Figure 5A,B), the population of CD86-positive cells in BM-iMG cells from the SOD1-tg group was significantly higher than the population from the wild-type group (see supplementary Figure 5C). With regard to mRNA expression, *Nos2* mRNA expression in BM-iMG cells from the SOD1-tg group was significantly higher than mRNA expression from the wild-type group, whereas the *Arg1* gene did not show a difference between the groups (see supplementary Figure 6A).

With regard to neuroprotection, the BM-iMG-conditioned medium from both the wild-type and SOD1-tg groups significantly protected against the cytotoxic effects of NOC-18; however, the effects seen with medium from the wild-type group were significantly superior to those observed with medium from the SOD1-tg group (see supplementary Figure 6B). These results suggested that the neuroprotective effects on motor neurons in BM-iMG cells from SOD1 mice were inferior to those in BM-iMG cells from wild-type mice. Therefore, the authors determined that it was better to use BM-iMG cells from wild-type mice for the treatment of ALS mice.

Therapeutic effects of transplantation of BM-iMG cells in SOD1-tg mice

The authors investigated the effect of BM-iMG cell transplantation in ALS model mice. BM-iMG cells generated from wild-type mice were transplanted into the spinal cords of 10-week-old SOD1-tg mice prior to the onset of ALS symptoms (Figure 4A–C), and analyses of several phenotypes, including body weight, motor function and longevity, were performed (Figure 4C). Regarding the safety of the procedure, no mice died shortly after transplantation. However, one mouse in the control group demonstrated >15% weight loss over a 1-week period 3 weeks after transplantation (13 weeks old), and one mouse in the BM-iMG group demonstrated >15% weight loss over a 1-week period 2 weeks after transplantation (12 weeks old). Therefore, these mice were excluded from the study, and 16 and 15 mice from the control and BM-iMG groups, respectively, were used for analysis.

The BM-iMG group showed a significant difference in inhibition of weight loss compared with the control group at 12–16 weeks of age (Figure 4D; also see supplementary Figure 7A). In a rotarod study, with the exception of the 4-week time point (14 weeks old), the BM-iMG group demonstrated a significant improvement 3–10 weeks after transplantation (13–20 weeks old) compared with the control group. The effect on motor function observed in the BM-iMG group was significant compared with that observed in the control group (Figure 4E; also see supplementary Figure 7B). At the endpoint, the BM-iMG group demonstrated a significant increase in overall survival and median survival time of as much as 2 weeks compared with the control group (Figure 4F).

Histochemical evidence of the anti-inflammatory effect of transplantation of BM-iMG cells in SOD1-tg mice

To investigate the mechanism of the therapeutic effect of BM-iMG cell transplantation, the authors performed an immunohistochemistry study focusing on neuronal cell loss and astrogliosis in the spinal cords of SOD1-tg mice 3 weeks after transplantation (13 weeks old) or at end stage (18–21 weeks old) (Figures 4C, 5). β3-tubulin and GFAP were used as markers for neurons and astrocytes, respectively. In immunostaining β3-tubulin at the anterior horn of the spinal cord, the authors demonstrated that neuronal cells were preserved in the BM-iMG cell transplantation group compared with the control group at the end of the experiment (Figure 5A). Quantitative analysis revealed that the number of β3-tubulin-positive cells decreased over time in the control group, with the number of β3-tubulin-positive cells in the BM-iMG group remaining significantly higher at end stage (Figure 5B). Although GFAP immunoreactivity increased over time in both the control and BM-iMG groups (Figure 5C–E), GFAP staining intensity and cell number in the BM-iMG group were significantly lower compared with the control group at end stage (Figure 5D,E). These results suggested that BM-iMG cells inhibit neuronal cell loss and astrogliosis in ALS.

To investigate the distribution and differentiation of transplanted BM-iMG cells, double immunofluorescence analysis was performed of GFP-positive cells (transplanted BM-iMG cells) and ionized calcium-binding adapter molecule 1 (Iba1) as microglia markers in the spinal cords of SOD1-tg mice at 3 weeks after transplantation (13 weeks old) or end stage (18–21 weeks old) (Figures 4B, 6). Three weeks after transplantation, GFP-positive BM-iMG cells were scattered in the spinal cords of the transplanted group and were positive for Iba1 staining. The number of Iba1-positive cells in the BM-iMG group was significantly higher than that in the control group, whereas the intensity of positive staining was not different between the two groups (Figure 6). Double-positive GFP and Iba1 cells were detected mainly at the injection site but were rarely present at end stage (Figure 6A). By contrast, at end stage, instead of GFP-positive cells, there was a massive migration of Iba1-positive/GFP-negative cells into the spinal cord over time in both the control and BM-iMG groups (Figure 6). Nevertheless, IBA1 signal intensity and cell number were significantly lower in the BM-iMG group than the control group at end stage (Figure 6B,C). These results strongly suggested that the transplantation of BM-iMG cells suppressed microglial activation through the indirect effects of BM-iMG cells (e.g., humoral factors).

Suppression of pro-inflammatory gene expression in SOD1-tg mice by transplantation of BM-iMG cells

Gene expression analysis was performed of the spinal cords of SOD1-tg mice at 3 weeks after transplantation (13 weeks old) or end stage (18–21 weeks old). *Nos2* and *Cd86* were analyzed as markers for pro-inflammatory microglia, whereas *Arg1* and *Mrc1* were analyzed as markers for neuroprotective microglia. The expression of *Nos2* in the BM-iMG group decreased significantly compared with that observed in the control group not only at end-stage but also at the age of 13 weeks (Figures 4A, 7). The expression of *Cd86* was comparable in the control and BM-iMG groups at both 13 weeks of age and end stage. By contrast, gene expression of *Arg1* and *Mrc1* significantly increased in the BM-iMG group compared with that observed in the control group at both 3 weeks after transplantation and end stage (Figure 7). Additionally, as the major inflammatory cytokines, the authors analyzed *Tnfα* and *Il-6* for gene expression. The expression level of *Tnfα* did not differ between the 3-week-after-transplantation and end-stage groups. However, the expression level of *Il-6* significantly decreased in the BM-iMG group compared with that observed in the control group at end stage only.

Discussion

Therapeutic research on ALS has been approached from various perspectives, including prevention and removal of the accumulation of denatured proteins, transplantation of biomaterials such as scaffolds and stem cells and administration of cytokines as immunomodulatory therapy [21–26]. Of note, the concept of “non-cell autonomous neuronal cell death” is a crucial point of view when

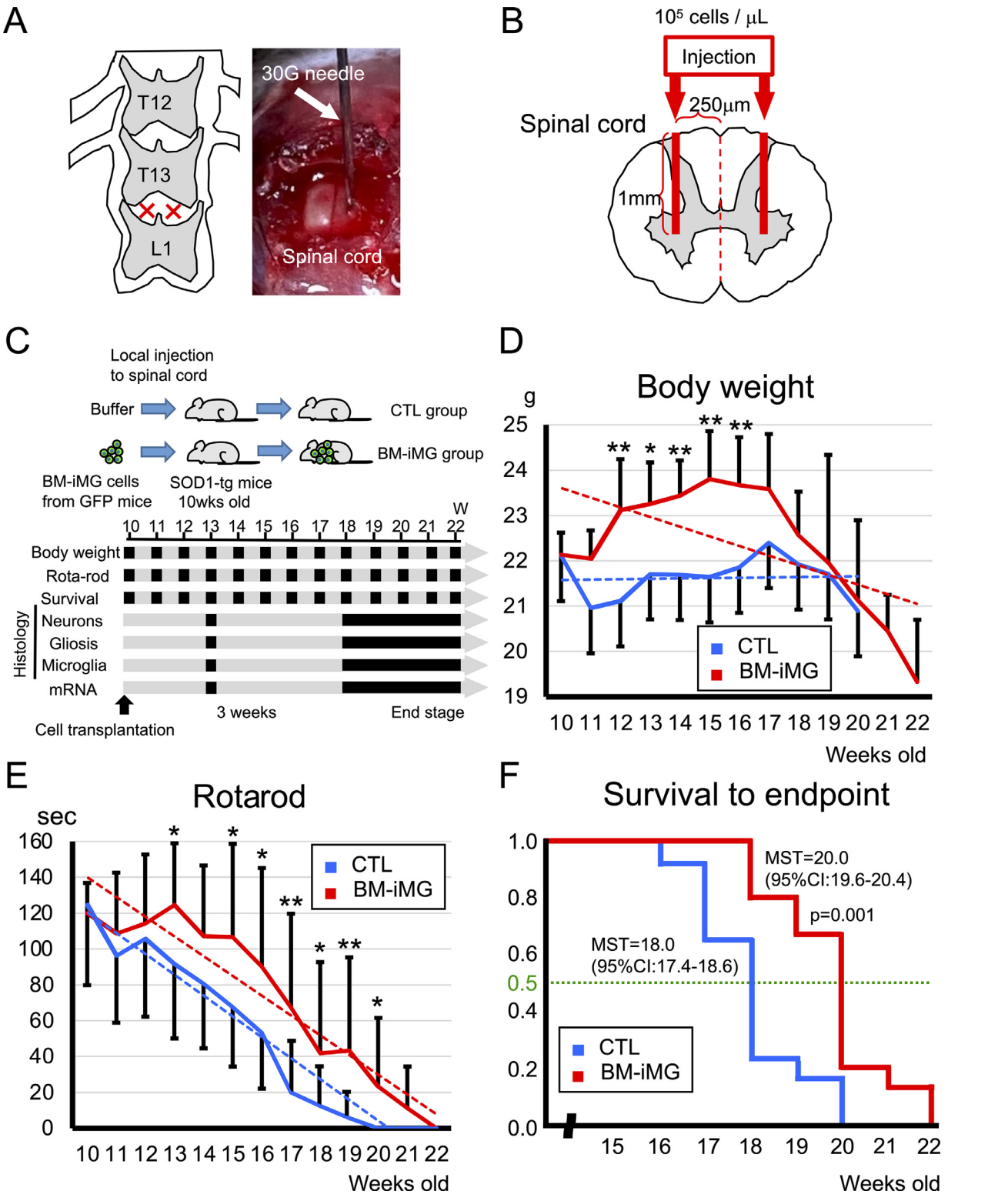

Figure 4. Effects of the transplantation of BM-iMG cells in SOD1-tg mice. (A) Location of injection for transplantation of BM-iMG cells into spinal cord. X marks between T13 and L1 vertebrae on bilateral sides of the spine show the points of needle insertion for transplantation. (B) Details of transplantation point for BM-iMG cells in the spinal cord. Each batch of 10^5 cells was injected 250 μm laterally from the midline of the spinal cord to a depth of 1 mm in bilateral sides. (C) Schematic experimental design. Transplantation of BM-iMG cells or CTL buffer was performed in male SOD1-tg mice at 10 weeks. Therapeutic effects were evaluated by body weight, rotarod test and survival ratio. In addition, histological and biological analyses were performed at the time point of each black bar in the time course. (D) Body weight was measured once a week from 10 weeks old to the end stage of the disease in the BM-iMG (red line) (n = 15) and CTL (blue line) (n = 16) groups. Red and blue dotted lines show a linear model of each group. (E) Rotarod test was performed once a week after transplantation of BM-iMG cells (red line) (n = 15) or administration of buffer (blue line) (n = 16). Red and blue dotted lines show a linear model of each group. Error bars show mean ± SD. (F) Kaplan–Meier curve of SOD1-tg mice in the BM-iMG (red line) (n = 15) and CTL (blue line) (n = 16) groups. Green dotted line shows median point. $^*P < 0.05$, $^{**}P < 0.01$. CI, confidence interval; CTL, control; G, gauge; MST, median survival time; SD, standard deviation; sec, seconds.

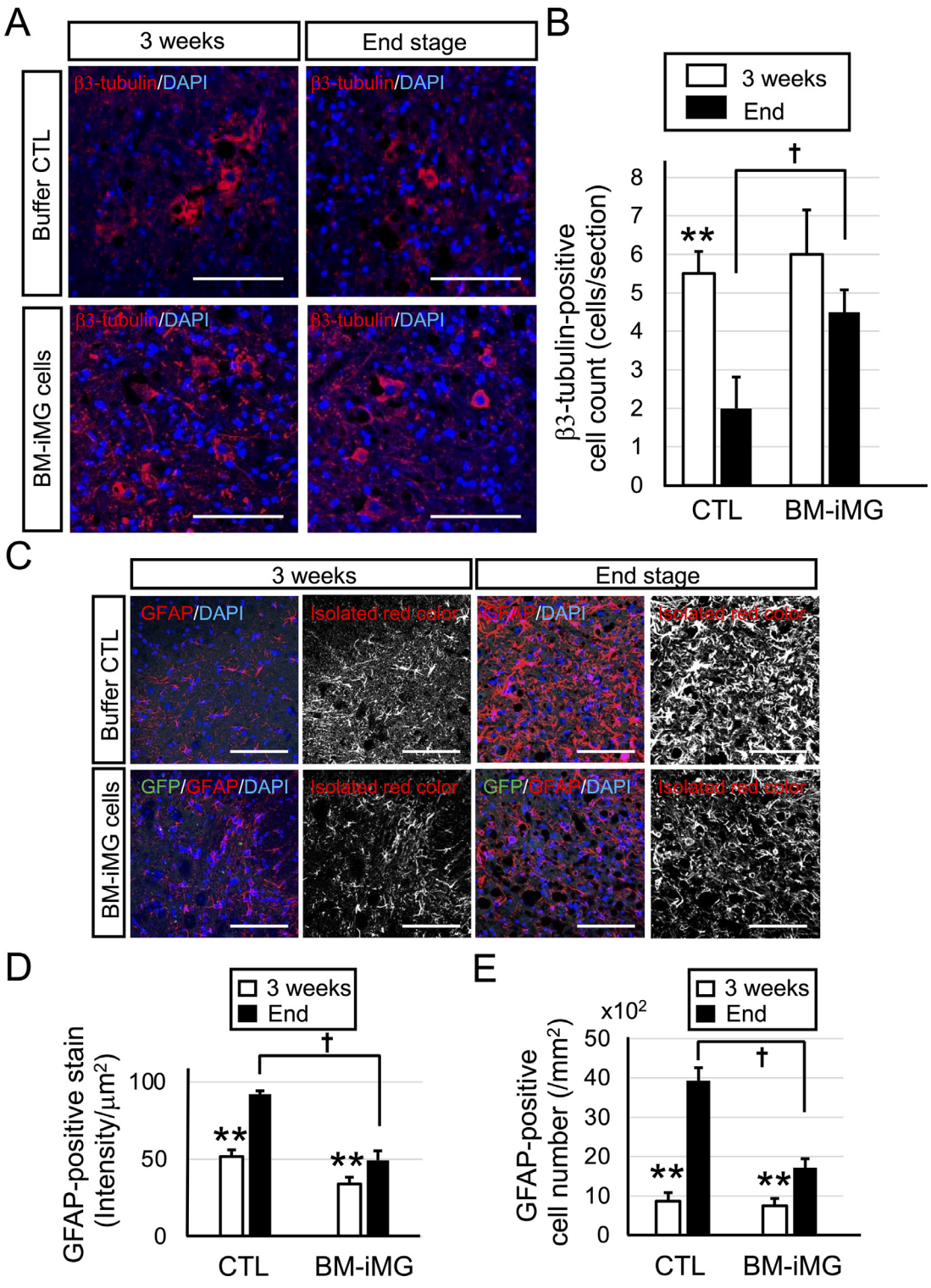

Figure 5. Histological analysis of spinal cords in SOD1-tg mice after transplantation therapy. (A) Immunohistochemistry of spinal cord with β-tubulin (red). Blue shows DAPI stain in nuclei. Scale bars = 100 μm. (B) β-tubulin-positive neurons were counted in anterior horn of spinal cord in BM-iMG and CTL groups (n = 5–7 in each group) at 3 weeks after transplantation and end stage. Scale bars = 100 μm. (C) Immunohistochemistry of spinal cord by GFAP antibody (red) with GFP signal (green) and nuclear stain (blue). Red color was isolated from merged pictures as GFAP-positive stain and is shown using black and white image. Scale bars = 100 μm. (D) GFAP-positive intensity of the black and white images was quantified and (E) GFAP-positive cell number was counted in spinal cords of SOD1-tg mice in the BM-iMG and CTL groups (n = 5–7 in each group) at 3 weeks after treatment and end stage. †$P < 0.01$, **$P < 0.01$ vs corresponding end stage group. CTL, control; DAPI, 4′,6-diamidino-2-phenylindole.

designing treatment strategies for ALS and various neurodegenerative diseases [27,28]. Motor neuron survival depends not only on internal conditions but also on the surrounding environment, such as glial cells and extracellular biochemical factors, including cytokines and neurotransmitters [29]. Therefore, any therapeutic strategy should pay cautious attention to the extra-motor neuron environment, which this study focused on.

Microglia are essential glial cells that play a crucial role in maintaining the CNS environment, and, similar to ALS, they are involved in the pathology of various diseases, including stroke, Parkinson

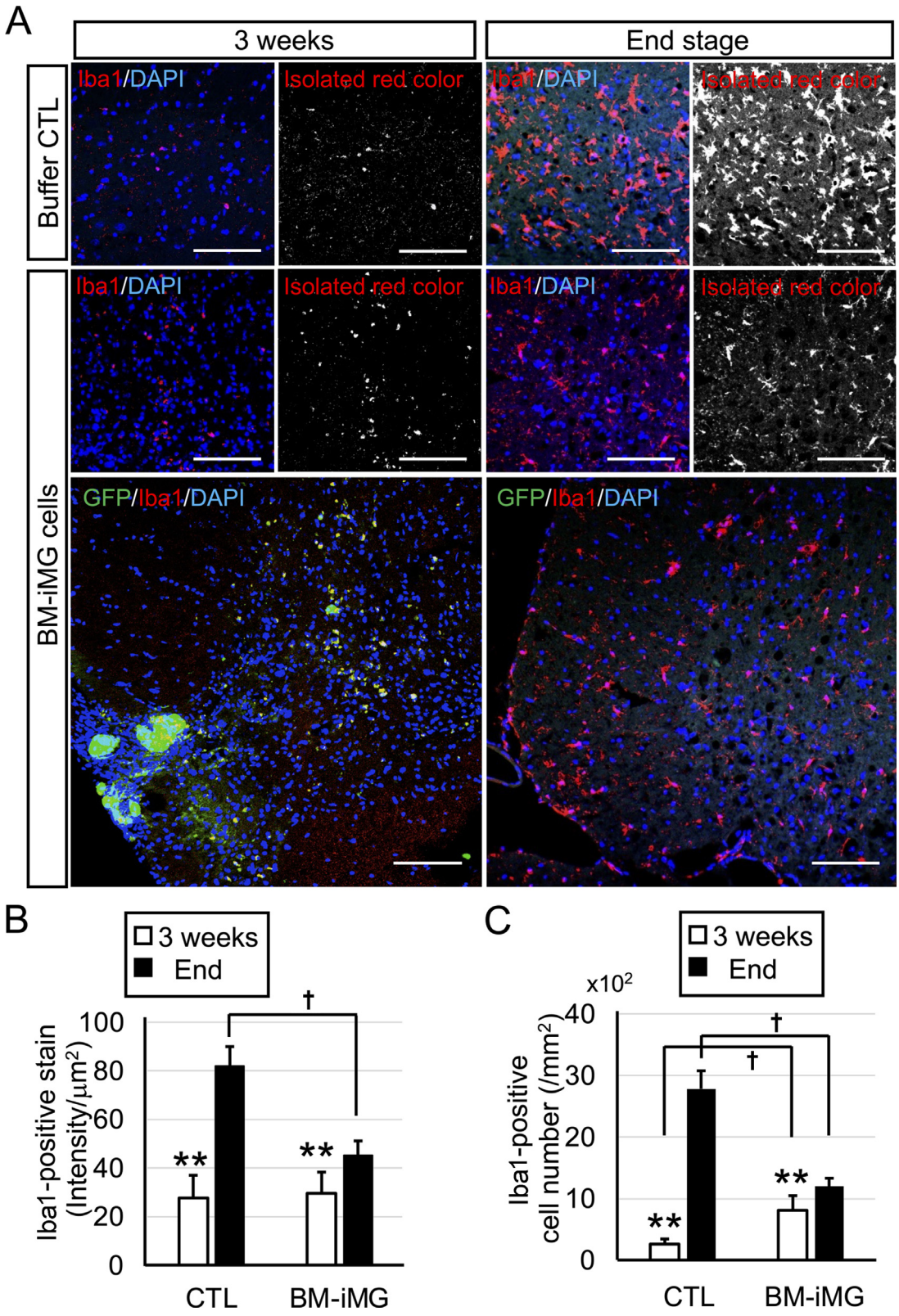

Figure 6. Histological analysisof microglia in the spinal cords of SOD1-tg mice after transplantation therapy. (A) Immunohistochemistry of Iba1 (red) with DAPI (blue) in the spinal cords of SOD1-tg mice at 3 weeks or end stage after transplantation and buffer administration. Red color was isolated from color pictures as Iba1-positive stain and is shown using black and white images. In large merged images, transplanted BM-iMG cells demonstrate a green color (GFP) in the spinal cords of SOD1-tg mice after transplantation therapy. Scale bars = 100 μm. (B) Bar graph shows the quantitative analysis of Iba1-positive stain and (C) Iba1-positive cell number in the spinal cords of SOD1-tg mice in the BM-iMG and CTL groups (n = 5–7 in each group) at 3 weeks after treatment or end stage. †$P < 0.01$, **$P < 0.01$ vs corresponding end stage group. CTL, control; DAPI, 4′,6-diamidino-2-phenylindole.

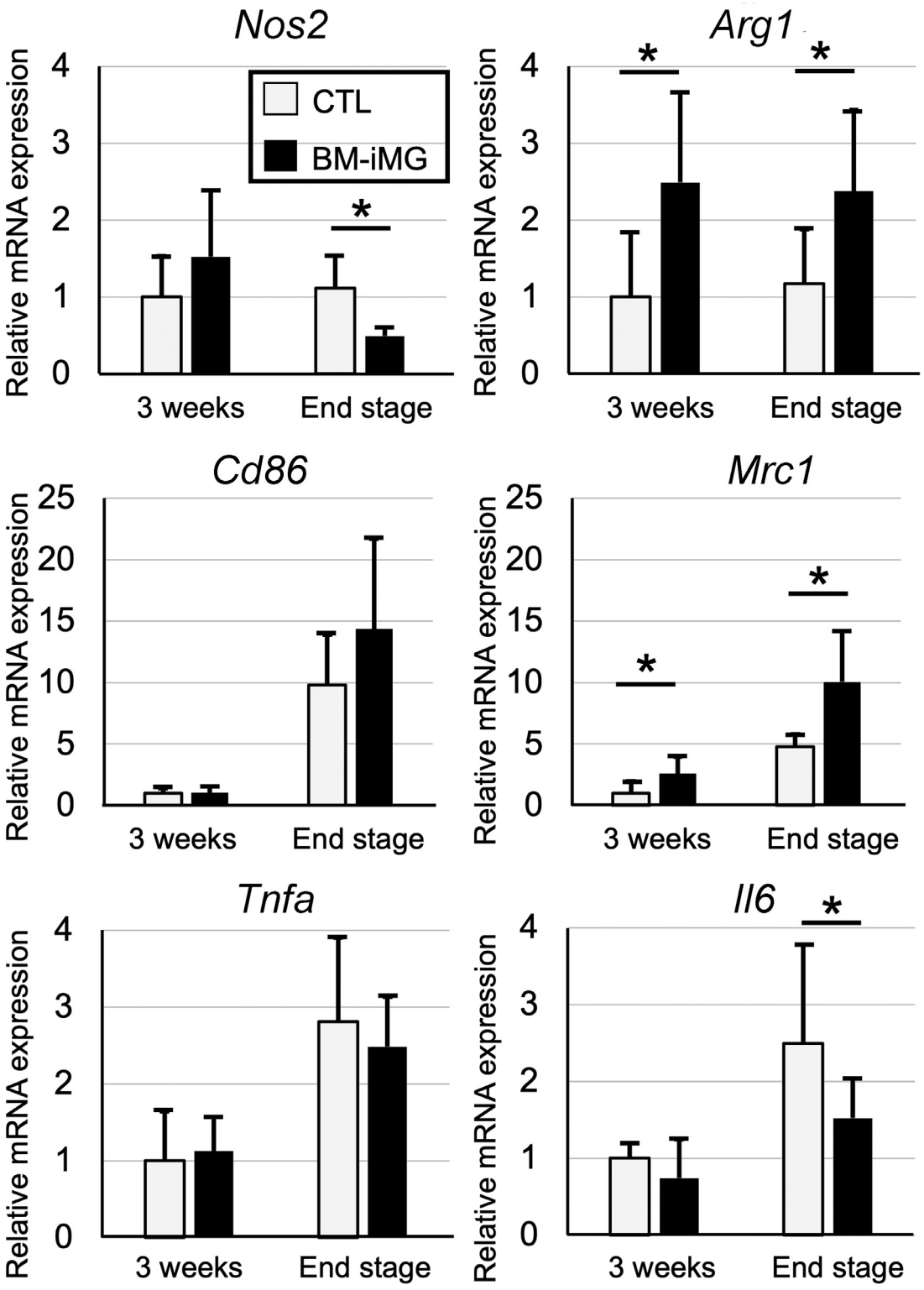

Figure 7. mRNA expression in the spinal cords of SOD1-tg mice after transplantation of BM-iMG cells. The relative mRNA expression of *Nos2, Arg1, Cd86, Mrc1, Tnfα* and *Il-6* was evaluated using spinal cords from SOD1-tg mice in the CTL and BM-iMG groups at 3 weeks and end stage. All data were normalized to *β*-actin mRNA expression. Error bars show mean ± SD (n = 5–7 in each group). *$P < 0.05$. CTL, control; SD, standard deviation.

disease and Alzheimer disease [8,9]. Microglia exhibit two opposite phenotypes, pro-inflammatory and neuroprotective, both of which are possibly associated with their functional differentiation and are implicated in the pathogenesis of various neurological disorders [10–13]. Recently, accumulating evidence has suggested that the same microglia exhibit both pro-inflammatory and neuroprotective phenotypes at different times depending on the disease condition rather than the presence of two separate phenotypes. Therefore, some researchers collectively refer to microglia under disease conditions as disease-associated microglia (DAM). Specifically, rather than clearly categorizing the function of microglia into two phenotypes, DAM has been described as the phenotype that changes

according to the stage of the disease; however, the details are still unclear [30]. Therefore, exogenous BM-iMG cells may exhibit characteristics that are different from those of DAM, which is present in pathological lesions. However, the therapeutic strategy of transplanting induced exogenous neuroprotective microglia at the site of injury or neurodegeneration should be warranted since BM-iMG cells have neuroprotective roles that include the therapeutic effects of microglial transplantation in neurological diseases, such as Alzheimer disease, stroke and spinal cord injury, as previously reported [20,31,32].

Neural stem cell transplantation has been conducted as a clinical trial of a presiding cell transplantation therapy for patients with ALS [33]. Moreover, the efficacy and safety of transplantation of human embryonic stem cell-derived astrocytes have been reported in an ALS mouse model [24]. These neurological cells seem to be appropriate for the treatment of neurological diseases. However, since they are derived from the human infant brain, immune rejection of allogeneic transplantation and ethical issues should be taken into account. Similarly, the human infant brain is required to prepare sufficient amounts of microglia for transplantation therapy, and highly technical and ethical hurdles are associated with this approach [34]. By contrast, the authors' study has a great advantage for the application of autologous transplantation by differentiation of bone marrow cells into therapeutic microglia *ex vivo*, as bone marrow cells are widely accepted as autologous transplantable cells [35]. Although immune cells derived from bone marrow have different origins and functions compared with those of the resident microglia in the brain [36], intervention into the myeloid lineage, such as bone marrow transplantation, has been shown in studies to offer a beneficial effect in ALS mice by inducing neuroprotective microglia-like cells [17–19,37]. Thus, in these studies, bone marrow-derived cells expressed *Iba1* as a microglia marker and neuroprotective cytokine and suppressed spinal cord inflammation by acting like microglia [17–19]. These lines of evidence prompted the authors to utilize the BM-MNCs contained in bone marrow-derived cells as candidate cells for inducing neuroprotective microglia, which were designated BM-iMG cells.

The authors successfully induced BM-iMG cells using GM-CSF and IL-4 as cytokines for the differentiation of bone marrow cells. GM-CSF differentiates bone marrow cells, such as hematopoietic stem cells and macrophage progenitors, into mature cells [38–40]. By contrast, IL-4 is the most classical cytokine, which induces differentiation into the neuroprotective microglia/macrophage phenotype and protects neuronal cells [41]. Here several combinations of these cytokines were tested to determine the induction efficiency of BM-iMG cells. Consequently, co-stimulation with GM-CSF and IL-4 following a single stimulation with GM-CSF was the best method for obtaining neuroprotective microglia-like cells with a phenotype of upregulated CD206 and ARG1 and downregulated inducible nitric oxide synthase.

By contrast, continuous co-stimulation with GM-CSF and IL-4 through the culture process slowed cell proliferation and resulted in insufficient induction of ARG1 and increased inducible nitric oxide synthase. The failure of this protocol might be due to the transdifferentiation effect of co-stimulation with GM-CSF and IL-4 in pre-differentiated BM-MNCs. Simultaneous treatment with GM-CSF and IL-4 is also popular for differentiating dendritic cells [42]. These results indicate that the timing and combination of administration of GM-CSF and IL-4 are critical.

In this study, engraftment of BM-iMG cells to the spinal cord was observed only 3 weeks after transplantation (albeit not at the end stage of the disease), which has also been described in several studies that have reported on the therapeutic effects of transplanted microglia [20,31,32]. Despite their short life span, transplanted BM-iMG cells demonstrated significant therapeutic effects in behavioral experiments for a longer time. Moreover, astrogliosis, neuronal loss and microglial proliferation were significantly suppressed at the end stage of the disease. In addition, the authors observed an upregulation of neuroprotective genes, such as *Arg1* and *Mrc1*, together with the downregulation of pro-inflammatory *Il-6*, even in the absence of engrafted cells. The reason why the neuroprotective effects exceeded the life span of engrafted BM-iMG cells is unclear. A possible explanation is the long-lasting humoral effects of protective molecules such as cytokines and extracellular vesicles from transplanted cells on the surrounding neurons and environment. The transplanted cells are expected to show the suppression of oxidative stress and neuroinflammation and the secretion of neuroprotective molecules in the spinal cord rather than to survive by engrafting in the host, which may result in improvement of the environment around neurons, induction of differentiation of surrounding cells and improvement of regenerative ability.

This study has several methodological limitations. First, the authors used BM-iMG cells from wild-type mice, rather than SOD1-tg mice, for the treatment of ALS mice because SOD1 BM-iMG cells are inferior to wild-type BM-iMG cells. Because of their mutant dismutase, SOD1 BM-iMG cells have a genetic disadvantage at the point of dismusing oxidative stress. These results may be consistent with familial ALS caused by mutant SOD1 but different for sporadic ALS. Therefore, for clinical application, the authors will attempt to induce BM-iMG cells and evaluate them in the bone marrow cells of ALS patients. Second, the authors employed an invasive method of direct injection of BM-iMG cells into the spinal cord; thus, the injection was limited to a single instance. Since bone marrow cells can be separated autologously, the authors' future mission is to develop an effective and safe method that will enable the authors to perform multiple administrations of BM-iMG cells to the spinal cord to augment and extend the effects.

Conclusions

The authors established a method for inducing neuroprotection of microglia-like cells from BM-MNCs. The authors demonstrated the therapeutic effects of spinal injection in ALS model mice. Since the authors' technical approach was based on easily accessible clinical procedures, such as isolation of bone marrow, technical optimization may accelerate clinical use in ALS patients in the future.

Funding

This study was supported by MEXT Kakenhi (grant nos. JP18K07498 and JP21K07413).

Declaration of Competing Interest

The authors have no commercial, proprietary or financial interest in the products or companies described in this article.

Author Contributions

Conception and design of the study: TT, MU, HK and MK. Acquisition of data: SK and TT. Analysis and interpretation of data: SK, TT and MU. Drafting or revising the manuscript: SK, TT and MU. All authors have approved the final article.

Acknowledgments

The authors thank the investigators at the Central Research Laboratory of Shiga University of Medical Science for their technical support.

Supplementary materials

Supplementary material associated with this article can be found in the online version at doi:10.1016/j.jcyt.2022.02.001.

References

[1] Westeneng H-J, Debray TPA, Visser AE, Van Eijk RPA, Rooney JPK, Calvo A, et al. Prognosis for patients with amyotrophic lateral sclerosis: development and validation of a personalised prediction model 2018;17:423.

[2] Mccauley ME, Baloh RH. Inflammation in ALS/FTD. Pathogenesis 2019;137:715–30.

[3] Troost D, van den Oord JJ, de Jong JM, Swaab DF. Lymphocytic infiltration in the spinal cord of patients with amyotrophic lateral sclerosis. Clin Neuropathol 1989;8:289–94.

[4] Engelhardt JI, Tajti J, Appel SH. Lymphocytic infiltrates in the spinal cord in amyotrophic lateral sclerosis. Arch Neurol 1993;50:30–6.

[5] Alexianu ME, Kozovska M, Appel SH. Immune reactivity in a mouse model of familial ALS correlates with disease progression. Neurology 2001;57:1282–9.

[6] Henkel JS, Beers DR, Zhao W, Appel SH. Microglia in ALS: the good, the bad, and the resting. J Neuroimmune Pharmacol Off J Soc NeuroImmune Pharmacol 2009;4:389–98.

[7] Boillée S, Yamanaka K, Lobsiger CS, Copeland NG, Jenkins NA, Kassiotis G, et al. Onset and progression in inherited ALS determined by motor neurons and microglia. Science 2006;312:1389–92.

[8] Saijo K, Glass CK. Microglial cell origin and phenotypes in health and disease. Nat Rev Immunol 2011;11:775–87.

[9] Salter MW, Stevens B. Microglia emerge as central players in brain disease. Nat Med 2017;23:1018–27.

[10] Kabba JA, Xu Y, Christian H, Ruan W, Chenai K, Xiang Y, et al. Microglia: Housekeeper of the Central Nervous System. Cell Mol Neurobiol 2018;38:53–71.

[11] Crain JM, Nikodemova M, Watters JJ. Microglia express distinct M1 and M2 phenotypic markers in the postnatal and adult central nervous system in male and female mice. J Neurosci Res 2013;91:1143–51.

[12] Ransohoff RM. A polarizing question: Do M1 and M2 microglia exist. Nat Neurosci 2016;19:987–91.

[13] Cherry JD, Olschowka JA, O'Banion MK. Neuroinflammation and M2 microglia: The good, the bad, and the inflamed. J Neuroinflammation 2014;11:98.

[14] Gao F, Chiu SM, Motan DAL, Zhang Z, Chen L, Ji H-L, et al. Mesenchymal stem cells and immunomodulation: current status and future prospects. Cell Death Dis 2016;7:e2062.

[15] Liao B, Zhao W, Beers DR, Henkel JS, Appel SH. Transformation from a neuroprotective to a neurotoxic microglial phenotype in a mouse model of ALS. Exp Neurol 2012;237:147–52.

[16] Zhang J, Liu Y, Liu X, Li S, Cheng C, Chen S, et al. Dynamic changes of CX3CL1/CX3CR1 axis during microglial activation and motor neuron loss in the spinal cord of ALS mouse model. Transl Neurodegener 2018;7:35.

[17] Terashima T, Kojima H, Urabe H, Yamakawa I, Ogawa N, Kawai H, et al. Stem cell factor-activated bone marrow ameliorates amyotrophic lateral sclerosis by promoting protective microglial migration. J Neurosci Res 2014;92:856–69.

[18] Terashima T, Kobashi S, Watanabe Y, Nakanishi M, Honda N, Katagi M, et al. Enhancing the Therapeutic Efficacy of Bone Marrow-Derived Mononuclear Cells with Growth Factor-Expressing Mesenchymal Stem Cells for ALS in Mice. IScience 2020;23:101764.

[19] Ohashi N, Terashima T, Katagi M, Nakae Y, Okano J, Suzuki Y, et al. GLT1 gene delivery based on bone marrow-derived cells ameliorates motor function and survival in a mouse model of. ALS. Sci Rep 2021;11:12803.

[20] Kobashi S, Terashima T, Katagi M, Nakae Y, Okano J, Suzuki Y, et al. Transplantation of M2-Deviated Microglia Promotes Recovery of Motor Function after Spinal Cord Injury in Mice. Mol Ther 2020;28:254–65.

[21] Tamaki Y, Shodai A, Morimura T, Hikiami R, Minamiyama S, Ayaki T, et al. Elimination of TDP-43 inclusions linked to amyotrophic lateral sclerosis by a misfolding-specific intrabody with dual proteolytic signals. Sci Rep 2018;8:6030.

[22] Abati E, Bresolin N, Pietro Comi G, Corti S. Preconditioning and Cellular Engineering to Increase the Survival of Transplanted Neural Stem Cells for Motor Neuron Disease Therapy. Mol Neurobiol 2019;56:3356–67.

[23] Kondo T, Funayama M, Tsukita K, Hotta A, Yasuda A, Nori S, et al. Focal transplantation of human iPSC-derived glial-rich neural progenitors improves lifespan of ALS mice. Stem Cell Reports 2014;3:242–9.

[24] Izrael M, Slutsky SG, Admoni T, Cohen L, Granit A, Hasson A, et al. Safety and efficacy of human embryonic stem cell-derived astrocytes following intrathecal transplantation in SOD1(G93A) and NSG animal models. Stem Cell Res Ther 2018;9:152.

[25] Abati E, Bresolin N, Comi G, Corti S. Advances, Challenges, and Perspectives in Translational Stem Cell Therapy for Amyotrophic Lateral Sclerosis. Mol Neurobiol 2019;56:6703–15.

[26] Rossi C, Cusimano M, Zambito M, Finardi A, Capotondo A, Garcia-Manteiga JM, et al. Interleukin 4 modulates microglia homeostasis and attenuates the early slowly progressive phase of amyotrophic lateral sclerosis. Cell Death Dis 2018;9:250.

[27] Beers DR, Henkel JS, Xiao Q, Zhao W, Wang J, Yen AA, et al. Wild-type microglia extend survival in PU.1 knockout mice with familial amyotrophic lateral sclerosis. Proc Natl Acad Sci U S A 2006;103:16021–6.

[28] Papadeas ST, Kraig SE, O'Banion C, Lepore AC, Maragakis NJ. Astrocytes carrying the superoxide dismutase 1 (SOD1G93A) mutation induce wild-type motor neuron degeneration *in vivo*. Proc Natl Acad Sci U S A 2011;108:17803–8.

[29] Mejzini R, Flynn LL, Pitout IL, Fletcher S, Wilton SD, Akkari PA. ALS Genetics, Mechanisms, and Therapeutics: Where Are We Now? Front Neurosci 2019;13:1310.

[30] Deczkowska A, Keren-Shaul H, Weiner A, Colonna M, Schwartz M, Amit I. Disease-Associated Microglia: A Universal Immune Sensor of Neurodegeneration. Cell 2018;173:1073–81.

[31] Zhu D, Yang N, Liu YY, Zheng J, Ji C, Zuo PP. M2 Macrophage Transplantation Ameliorates Cognitive Dysfunction in Amyloid-β-Treated Rats Through Regulation of Microglial Polarization. J Alzheimers Dis 2016;52:483–95.

[32] Kanazawa M, Miura M, Toriyabe M, Koyama M, Hatakeyama M, Ishikawa M, et al. Microglia preconditioned by oxygen-glucose deprivation promote functional recovery in ischemic rats. Sci Rep 2017;7:42582.

[33] Mazzini L, Gelati M, Profico DC, Sorarù G, Ferrari D, Copetti M, et al. Results from Phase I Clinical Trial with Intraspinal Injection of Neural Stem Cells in Amyotrophic Lateral Sclerosis: A Long-Term Outcome. Stem Cells Transl Med 2019;8:887–97.

[34] Dello Russo C, Cappoli N, Coletta I, Mezzogori D, Paciello F, Pozzoli G, et al. The human microglial HMC3 cell line: where do we stand? A systematic literature review. J Neuroinflammation 2018;15:259.

[35] Chu D-T, Phuong TNT, Tien NLB, Tran DK, Van Thanh V, Quang TL, et al. An Update on the Progress of Isolation, Culture, Storage, and Clinical Application of Human Bone Marrow Mesenchymal Stem/Stromal Cells. Int J Mol Sci 2020;21:708.

[36] Ginhoux F, Lim S, Hoeffel G, Low D, Huber T. Origin and differentiation of microglia. Front Cell Neurosci 2013;7:45.

[37] Corti S, Locatelli F, Donadoni C, Guglieri M, Papadimitriou D, Strazzer S, et al. Wild-type bone marrow cells ameliorate the phenotype of SOD1-G93A ALS mice and contribute to CNS, heart and skeletal muscle tissues. Brain 2004;127:2518–32.

[38] Hamilton JA. GM-CSF in inflammation and autoimmunity. Trends Immunol 2002;23:403–8.

[39] Lee SC, Liu W, Brosnan CF, Dickson DW. GM-CSF promotes proliferation of human fetal and adult microglia in primary cultures. Glia 1994;12:309–18.

[40] Boche D, Perry VH, Nicoll JAR. Review: Activation patterns of microglia and their identification in the human brain. Neuropathol Appl Neurobiol 2013;39:3–18.

[41] Pepe G, De Maglie M, Minoli L, Villa A, Maggi A, Vegeto E. Selective proliferative response of microglia to alternative polarization signals. J Neuroinflammation 2017;14:236.

[42] Gluckman JC, Canque B, Chapuis F, Rosenzwajg M. *In vitro* generation of human dendritic cells and cell therapy. Cytokines Cell Mol Ther 1997;3:187–96.